# Image Reconstruction Algorithm for a SPECT System with a Convergent Rotating Slat Collimator

Gengsheng L. Zeng
University of Utah, Salt Lake City, UT 84108, USA
Daniel Gagnon
Marconi Medical Systems, Cleveland, OH 44143, USA

***Abstract*** — In this paper we suggest the use of a convergent rotating slat collimator in a SPECT system that contains strip-shaped CdZnTe detectors. This imaging device is able to provide high spatial and energy resolution for small animal imaging. A novel design method and reconstruction technique are proposed for use in this system.

## I. Introduction

A parallel, slat collimator shown in Figure 1 was proposed in 1975 by Keyes [1]. This collimator can be mounted on a gamma camera for SPECT (single photon emission computed tomography) imaging. This collimator does not consist of holes. Instead, it is made of parallel plates. One advantage of a slat collimator over a hole collimator is its better geometric efficiency [4]-[7]. However, this slat collimator can only measure a one-dimensional profile, and therefore cannot be used to directly measure a two dimensional image. A planar image can only be reconstructed using one-dimensional profiles. Three-dimensional imaging requires two motions: Collimator rotation and detector rotation as illustrated in Figure 1.

The idea of using a rotating collimator was later adopted in applications of semiconductor detectors [2][3] and NaI(Tl) Anger cameras [4]-[7].

In this paper we propose using a convergent rotating slat collimator for SPECT, and the development of a reconstruction algorithm.

This research is directed towards building a small animal SPECT imager with both high spatial resolution and excellent energy resolution. CdZnTe semiconductor chips have been used to build a gamma ray detector [8][9]. The detector is strip-shaped, like the detector depicted in Figure 1. However, the collimation slats are arranged so that they have a focal line in front of the detector, as illustrated in Figure 2. This design enables us to achieve a sub-millimeter spatial resolution. The distance between the focal line and the detector is referred to as the collimator's *focal length*. The focal length will be determined by the object size. A smaller object requires a shorter focal length.

## II. Methods

### *A. Projection data*

A common feature of slat collimator is that the measured projection is a weighted planar integral rather than a line integral.

Let's first assume that the detector is infinitely narrow. We have an approximate "point detector" between adjacent collimator slats. The planar integral that this point detector measures is weighted by a factor of $1/r$, where $r$ is the distance between the point detector and the point-object.

If the detector is not narrow, we can treat it as rows of independent point detectors, each one having its own weighting factor of $1/r_i$. The integrated effect of each factor $1/r_i$ yields a distance dependent weighting factor in the planar integral. The measured projection value is the sum of all measurements from a row of individual "point-detectors." The goal behind this work is to develop a method to remove the $1/r_i$ weighting factor from each "point-detector."

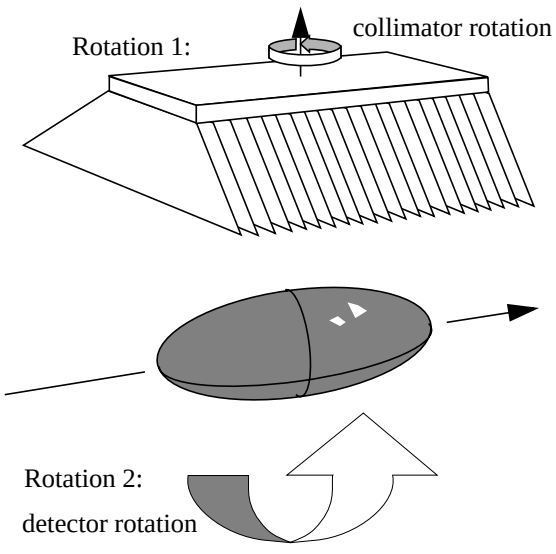


Figure 1. A Parallel rotating slat collimator

### *B. Introduction of a small tilt angle*

In order to remove the $1/r_i$ weighting factor from the projection data, we modified the convergent slat collimator shown in Figure 2 by tilting every slat a small angle δ, as indicated by the broken lines in Figure 3.

### *C. Algorithm*

Let us consider the local coordinate system shown in Figure 4. This local coordinate system is centered at an arbitrary "point-detector" which measures a weighted planar integral of the plane labeled **a**. Since the collimator slats are tilted by a small angle δ, after the collimator rotates 180˚ (Rotation 1 in Figure 1), another "point-detector" will be rotated to the location where the previous "point-detector" was located. The new "point-detector" measures a weighted planar integral of the plane labeled **a'**. If plane **a** is tilted *up* by a small angle δ, then plane **a'** is tilted *down* by a small angle δ.

The measurement at plane **a** is given as

$$g(\delta) = \iint \frac{1}{r} f(r, \alpha, r\tan\delta) r\,dr\,d\alpha \qquad (1)$$

and the measurement at plane **a'** is given as

$$g(-\delta) = \iint \frac{1}{r} f(r, \alpha, -r\tan\delta) r\,dr\,d\alpha . \qquad (2)$$

By subtracting Eq. (2) from Eq. (1) and multiplying the difference by a constant $(\cos^2\delta)/(2\delta)$, we have

$$\frac{g(\delta) - g(-\delta)}{2\delta}(\cos^2\delta) \qquad (3)$$

$$= \frac{\iint \frac{1}{r} f(r, \alpha, r\tan\delta) r\,dr\,d\alpha - \iint \frac{1}{r} f(r, \alpha, -r\tan\delta) r\,dr\,d\alpha}{2\delta}.$$

Equation (3) can also be expressed as:

$$\frac{g(\delta) - g(-\delta)}{2\delta}(\cos^2\delta) \qquad (4)$$

$$= \iint \frac{1}{r} \frac{f(r, \alpha, r\tan\delta) - f(r, \alpha, -r\tan\delta)}{2\delta} r\,dr\,d\alpha .$$

The $\frac{f(r, \alpha, r\tan\delta) - f(r, \alpha, -r\tan\delta)}{2\delta}$ portion of Eq. (4) is readily recognized as an approximation of the partial derivative of $f$, with respect to variable δ, and multiplied by a constant $\frac{r}{\cos^2\delta}$, because

$$\frac{d}{d\delta} r\tan\delta = \frac{r}{\cos^2\delta} . \qquad (5)$$

Using the local coordinate system presented in Figure 4, and recognizing the fact that the $r$'s in $r/\cos^2\delta$ and $1/r$ cancel out, we have:

$$\iint \frac{\partial}{\partial w} f(r, \alpha, w) r\,dr\,d\alpha = \frac{\partial}{\partial w} \iint f(r, \alpha, w) r\,dr\,d\alpha \qquad (6)$$

and

$$\frac{g(\delta) - g(-\delta)}{2\delta}(\cos^2\delta) \qquad (7)$$

$$\approx \iint \frac{\partial}{\partial w} f(r, \alpha, w) r\,dr\,d\alpha$$

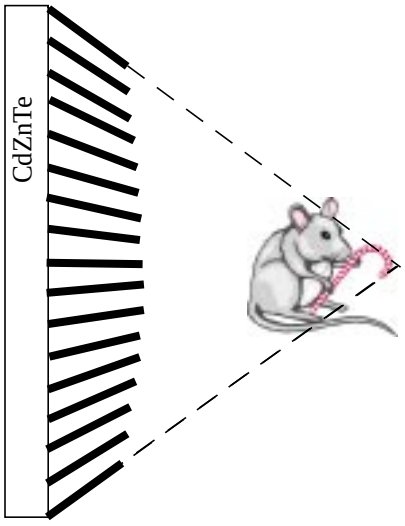


Figure 2. A convergent collimator.

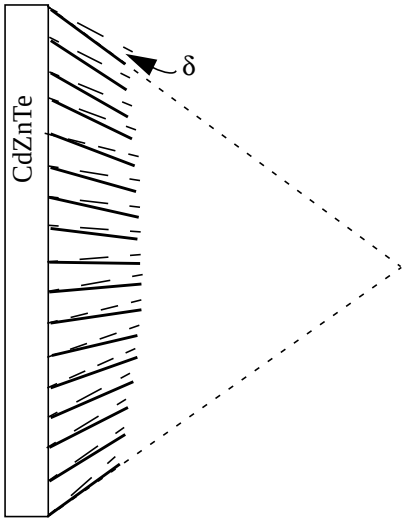


Figure 3. A convergent collimator with a small tilt-angle δ.

$$= \frac{\partial}{\partial w}\iint f(r,\alpha,w)\,r\,dr\,d\alpha .$$

Here, $\iint f(r,\alpha,w)\,r\,dr\,d\alpha$ is the Radon transform of object *f*.

The Radon inversion formula reconstructs the image $f$ by backprojecting the second-order derivative of the Radon transform, i.e., by backprojecting $\frac{\partial^2}{\partial w^2}\iint f(r,\alpha,w)\,r\,dr\,d\alpha$.

The reconstruction procedure is as follows:

i) Measure data at plane **a**, see Eq. (1).

ii) Rotate the collimator 180° and measure data at plane **a'**, see Eq. (2).

iii) Take the difference of the above two measurements and normalize it by a constant $(\cos^2\delta)/(2\delta)$, See Eq. (7). [Note: This step could also be the very last step in the reconstruction, because $(\cos^2\delta)/(2\delta)$ is a constant.]

iv) Sort the data according to the detector orientation, then store the data in the Radon space.

v) Take the derivative of the data along the radial direction in the Radon space, obtaining the second-order derivative of the Radon transform.

vi) Backproject the data according to the Radon inversion formula:

$$f(\vec{x}) = -\frac{1}{8\pi}\int_0^{\pi}\int_0^{\pi} p''_{\theta\varphi}(\vec{x}\cdot\hat{\theta})\sin\theta\,d\theta\,d\varphi \qquad (8)$$

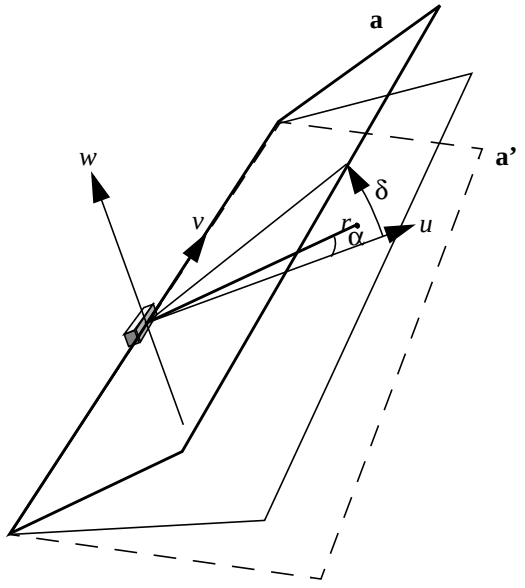


Figure 4. Local coordinate systems: The cylindrical system $(r,\alpha,w)$ and the Cartesian system $(u,v,w)$.

where $\vec{x}$ is a point in the 3D image space and $\hat{\theta}$ is the direction of the detector, which is the *w* direction in Figure 4. The angle $\theta$ is the angle of Rotation 1 indicated in Figure 1 and $\theta = 0°$ corresponds to the position where $\hat{\theta}$ is parallel to the axis of Rotation 2. The angle $\varphi$ is determined by Rotation 2 and the starting angle is arbitrary. The Radon transform of the object *f* is denoted by *p*, and

$$p'' = \frac{\partial^2}{\partial w^2}\iint f(r,\alpha,w)\,r\,dr\,d\alpha . \qquad (9)$$

### *D. Data sufficiency condition*

In order to guarantee a sufficient measurement of the data, we require that every point $\vec{x}$ in the region-of-interest should see a backprojected plane from *ALL* orientations.

Let us define the *focal point* of the collimator to be the point directly in front of the detector center on the focal line. To obtain a sufficient data measurement, the focal point position must have a non-planar trajectory. Figure 5 illustrates two examples that can be used to acquire a complete data set.

## III. Discussion

In this paper we outlined the development of a reconstruction method for SPECT imaging utilizing a convergent rotating slat collimator. The method introduced a small tilt-angle for the slats and a differential technique to remove the 1/*r* weighting factor

in the projection data, which were then converted into Radon data. The Radon inversion formula was used to reconstruct the image. A data sufficiency condition for this imaging geometry was also discussed.

## IV. References


1. Keyes W. I., "The fan-beam gamma camera," Phys. Med. Biol. 20, 489-491 (1975).
2. Urie M. M., Mauderli W., Fitzgerald L. T., and Williams C. M., "Rotating laminar emission camera with GE-detector," *IEEE Trans. Nucl. Sci.* 26, 552-558 (1979).
3. Mauderli W., Luthmann R. W., Fitzgerald L. T., Urie M. M., Williams C. M., Tosswill C. H., and Entine G., "A computerized rotating laminar radionuclide camera," *J. Nucl. Med*. 20, 341-344 (1979).
4. Lodge M. A., Binnie D. M., Flower M. A., and Webb S., "The experimental evaluation of a prototype rotating slat collimator for planar gamma camera imaging," *Phys. Med. Biol*. 40, 427-448 (1995).
5. Lodge M. A., Webb S., Flower M. A., and Binnie D. M., "A prototype rotating slat collimator for single photon emission computed tomography," *IEEE Trans. Med. Imaging*, 15, 500-511 (1996).
6. Webb S., Binnie D. M., Flower M. A., and Ott R. J., "Monte Carlo modelling of the performance of a rotating slit-collimator for improved planar gamma-camera imaging," *Phys. Med. Biol*. 37, 1095-1108 (1990).
7. Webb S., Flower M. A., and Ott R. J., "Geometric efficiency of a rotating slit-collimator for improved planar gamma-camera imaging," *Phys. Med. Biol.* 38, 627-638 (1993).
8. Matherson K. J., Barber H. B., Barrett H. H., Eskin J. D., Dereniak E. L., Woolfenden J. M., Young E. T., and Augustine F. L., "Progress in the development of large-area modular 64 x 64 CdZnTe imaging arrays for nuclear medicine," *IEEE Trans. Nucl. Sci*. 45, 354-358 (1988).
9. Butler J. F., Lingren C. L., Friesenhahn S. J., Doty F. P., Ashburn W. L., Conwell R. L., Augustine F. L., Apotovsky B., Pi B., Collins T., Zhao S., and Isaacson C., "CdZnTe solid-state gamma camera," *IEEE Trans. Nucl. Sci*. 45, 359-363 (1998).


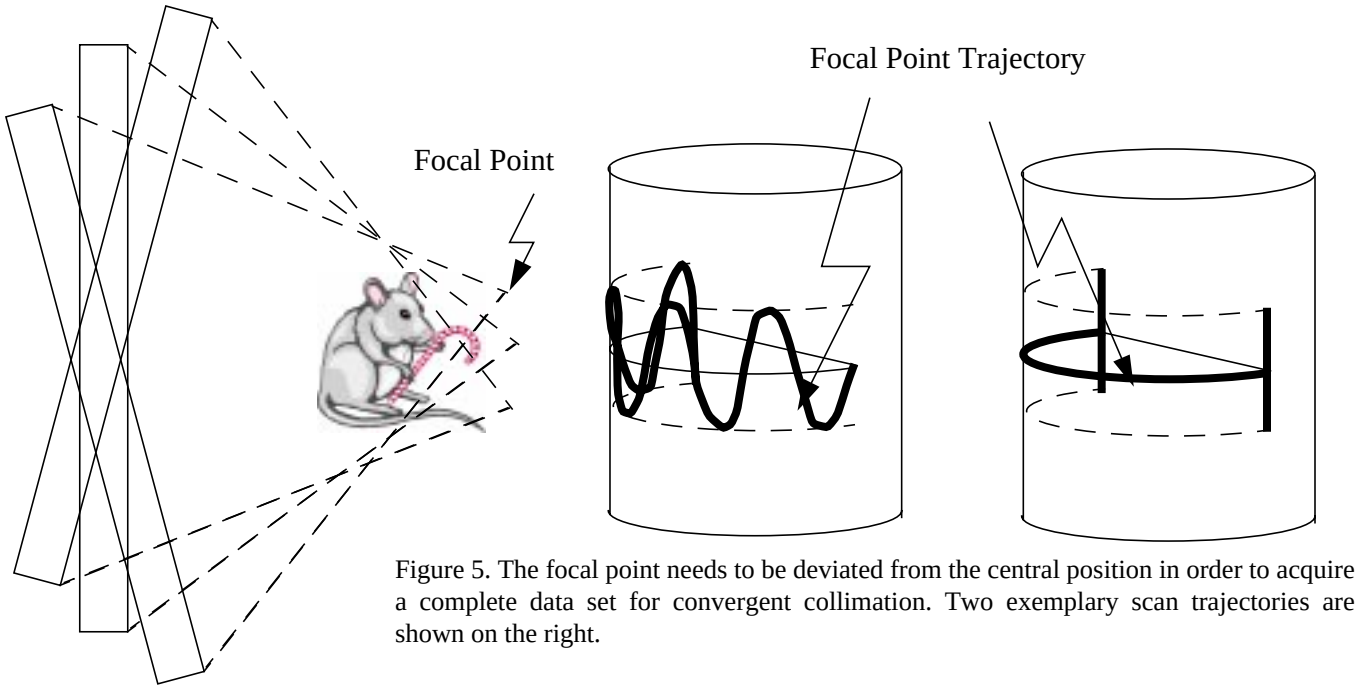


Figure 5. The focal point needs to be deviated from the central position in order to acquire a complete data set for convergent collimation. Two exemplary scan trajectories are shown on the right.